

Electrohydrodynamic transport of ozone in a corona radical shower non-thermal plasma reactor

J. MIZERACZYK, J. PODLIŃSKI, M. DORS, M. KOCIK

*Institute of Fluid Flow Machinery, Polish Academy of Sciences,
Fiszera 14, 80-231 Gdańsk, Poland, e-mail: jmiz@imp.gda.pl*

T. OHKUBO, S. KANAZAWA

*Dept. of Electrical and Electronic Engineering, Oita University,
700 Dannoharu, Oita 870-1192, Japan*

J. S. CHANG

*Dept. of Engineering Physics, McMaster University,
Hamilton, Ontario, L8S 4M1 Canada*

Received 20 April 2002

In this paper results of the experimental investigation of ozone molecule transport along a corona discharge radical shower (CDRS) non-thermal plasma reactor are presented. The measured axial ozone concentration distributions along the CDRS reactor show that the ozone molecules produced in the discharge region were transported from their origin both in the upstream and downstream regions of the CDRS reactor, i.e. also against the main gas flow. The images of the flow structures in the CDRS reactor suggests that the electrohydrodynamic (EHD) flow is responsible for the ozone transport upstream.

PACS: 52.80.Hc

Key words: corona discharge, ozone transport, non-thermal plasma

1 Introduction

Recently, Ohkubo et al. [1] and Kanazawa et al. [2] found that the removal of NO molecules in a needle-to-plate and corona discharge radical shower (CDRS) non-thermal plasma reactors occurred not only in the streamer corona discharge and downstream regions of the reactors but also in the reactor upstream region. The reason of the NO removal in the upstream region of the reactor is not clear at this moment. However, the results of the previous (e.g. [3-5]) and recent (e.g. [6, 7]) experiments on the electrohydrodynamic (EHD) secondary flow (ionic wind) in electrostatic precipitator models suggest that the EHD flow is capable of transporting long-living active species upstream of the discharge region, where they may react with other species. Hence, if the ozone molecules were transported by the EHD flow upstream of the discharge region in the experiment of Ohkubo et al. [1] and Kanazawa et al. [2], they would be long-live and active enough to oxidize NO molecules and efficiently remove them before they reach the discharge region.

In this paper we present results of the investigation of ozone molecule transport along a CDRS non-thermal plasma reactor. In addition to the fundamental interest

in the transport of ozone and other species transport in the non-thermal plasma reactors, this investigation is related to one of the most topical questions of the non-thermal plasma technology for gaseous pollutant abatement: how (if at all) the corona discharge itself and the no-discharge region (the part of the reactor not covered by the discharge) are involved in the reduction and/or oxidation of the gaseous pollutants in the non-thermal plasma reactors.

2 Experimental apparatus

A schematic diagram of the experimental apparatus is shown in Fig. 1. The reactor was an acrylic box (100 mm × 200 mm × 1000 mm). A stainless-steel pipe (4 mm in diameter) with 18 stainless-steel nozzle electrodes (1.5 mm outer diameter, 1 mm inner diameter, 5 mm length), soldered into the pipe as shown in Fig. 2, was used as a CDRS electrode. It was mounted in the middle of the reactor, in halfway between two grounded parallel plate stainless-steel electrodes (200 mm × 600 mm). Positive polarity DC high voltage was applied through a 10 MΩ resistor to the pipe with nozzle electrodes. The operating voltage was varied from 0 to 31 kV to develop a stable streamer corona discharge from each nozzle to the plate electrodes.

Two gas flows, the main and the additional, were established in the reactor. The main gas (ambient air) flowed along the reactor, driven by an induced fan. The average velocity of the main gas flow was varied from 0.18 to 0.8 m/s. This is a range typical for electrostatic precipitators operations. The additional gas (N₂ : O₂ : CO₂ = 80% : 5% : 15%) was injected through the nozzles into the main gas flow with a flow rate varied from 0.25 to 1.5 l/min (gas velocity at the nozzle outlet was 0.3–1.8 m/s). The presence of CO₂ (15%) stabilized streamer corona discharge mode, preventing glow and spark discharge modes [11].

Concentration of ozone, produced by the streamer corona discharge, was measured along the reactor on the x axis placed 1 cm below the discharge electrode (Fig. 1), using a cylindrical plastic sampling probe (1 mm in diameter), through which the operating gas was sucked into a calibrated FTIR spectrophotometer having a long-path measuring cell. The suction was very slow (a suction rate was 2.25 cm³/s), hence, it disturbed the flow fairly weak. As tested, a lower suction rate gave similar measuring results. The experiment was run at room temperature under atmospheric pressure.

Flow structures in the CDRS reactor were visualized to elucidate the mechanism of ozone transport into the upstream region of the reactor. Using a CuBr laser ($\lambda = 510.6$ nm and $\lambda = 578.2$ nm) [12], the so-called laser sheet of a thickness of 1 mm, formed by a telescope, was set along the reactor, perpendicularly to the electrode. Seed particulate (cigarette smoke), which followed the flow, was added either to the main or additional gas for scattering the laser-sheet light. The images of the particulates moving with the flow in the laser sheet were recorded with a video camera, and acquired with a computer.

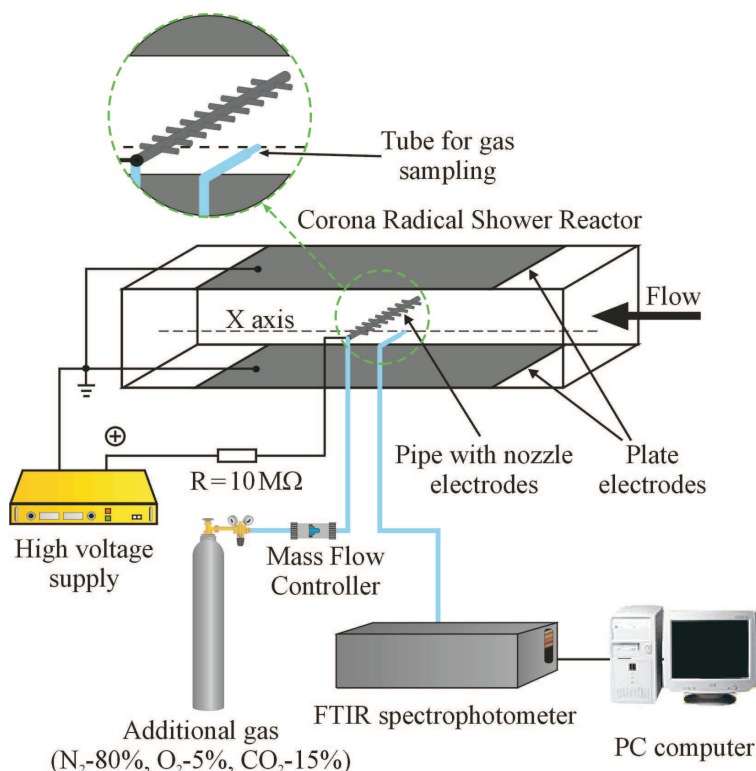


Fig. 1. Experimental set-up.

3 Experimental results

3.1 Spatial distribution of ozone concentration

In general, the ozone molecules, produced around the electrodes during the streamer corona discharge, can be transported from their origin both downstream and upstream of the discharge region due to the diffusion, additional gas flow from all the nozzles and electrohydrodynamic (EHD) secondary flow. They are also transported by convection of the main gas flow, but only downstream. When a steady state is established in the CDRS reactor, spatial distributions of the ozone molecules are settled as a net effect of the ozone production and transport.

Fig. 2 shows the steady-state ozone concentration distributions along the CDRS reactor for various main gas flow velocities ranged from 0.18 to 0.8 m/s. As it is seen from Fig. 2, ozone molecules are present in both the downstream and upstream regions of the CDRS reactor, assuming the position of the discharge electrode as a reference. Except for the lowest main gas velocity (0.18 m/s), the ozone concentration exhibits a maximum around the discharge zone (due to the ozone production) and decreases when moving upstream regardless of main gas flow velocities. At main

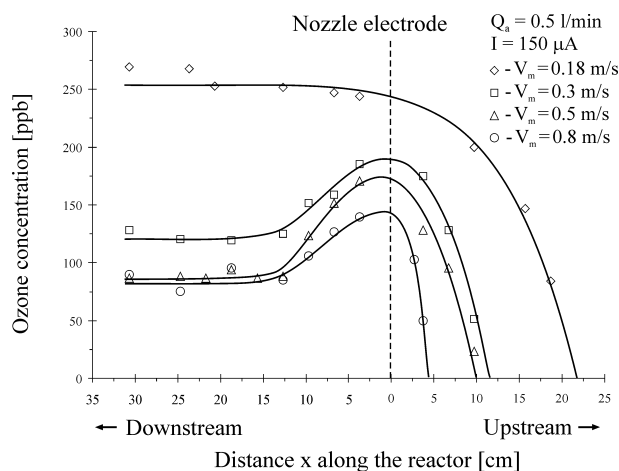


Fig. 2. Ozone concentration distribution along the CDRS reactor during the positive DC streamer corona discharge for various main gas (air) flow velocities V_m . The ozone concentrations were measured along x axis, placed along the reactor 1 cm below the discharge electrode (Fig. 1). Additional gas [$\text{N}_2(80\%) : \text{O}_2(5\%) : \text{CO}_2(15\%)$] flow rate $Q_a = 0.5$ l/min, averaged discharge current $I = 150 \mu\text{A}$.

gas flow velocities higher than 0.18 m/s, the ozone concentration decreases downstream and then, when the convection by the main gas flow becomes dominant, is constant. At the lowest main gas flow velocity tested (0.18 m/s), the ozone concentration distribution around the discharge zone is apparently governed more or less equally by the diffusion, main gas convection and EHD flow, hence, it does not exhibit downstream any decrease. The ozone penetration length upstream depends on the main gas flow velocity. It is shorter at higher main gas flow velocities because the role of the main gas convection in the ozone molecule transport increases. The ozone molecules are found in the upstream region of the CDRS as deep as about 20 cm from the discharge electrode at a main gas flow rate of 0.18 m/s. At a main gas flow rate of 0.8 m/s, the ozone molecules penetrate upstream only a few cm.

3.2 Test on the additional gas penetration into the upstream region (without discharge)

In order to experimentally estimate the penetration of the additional gas into the upstream region of the CDRS reactor without discharge, we measured the axial distributions of concentration of N_2O or CH_4 (chosen as easy to detect) blown through the nozzles into the reactor as an additional gas at various main gas (air) flow velocities. The additional gas concentration distributions were measured similarly as the ozone concentration in the experiment described in 3.1. The results are shown in Fig. 3.

As it is seen from Fig. 3, N_2O and CH_4 molecules were not found in the upstream region (more correctly on the x -axis upstream, see Fig. 2). Their transport into the

upstream region due to the diffusion (the diffusion coefficients are $D_1 = 0.15 \text{ cm}^2 \text{ s}^{-1}$ and $D_2 = 0.213 \text{ cm}^2 \text{ s}^{-1}$ for N_2O and CH_4 , respectively, [19]) and additional flow is weaker than that downstream due to the convection by the main gas. Therefore, we may infer that also in the case of ozone the main gas convection is stronger than the ozone diffusion and additional flow transport. Hence, the ozone presence in the CDRS reactor upstream cannot be explained by those two factors.

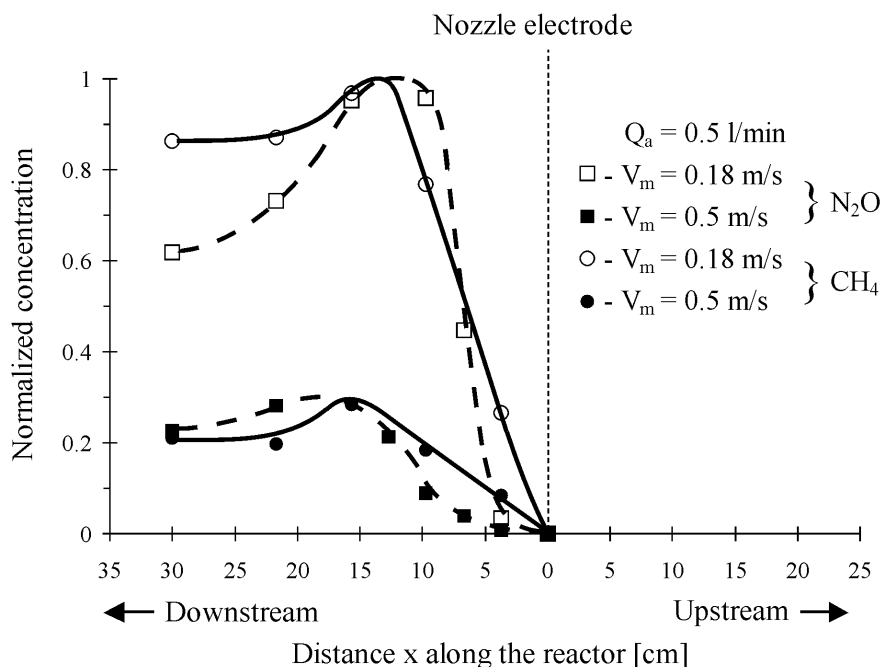


Fig. 3. N_2O and CH_4 concentrations along the CDRS reactor (without discharge) for various main gas (air) flow velocities V_m . The concentrations were measured along x axis, placed along the reactor 1 cm below the discharge electrode (Fig. 1). Additional gas (N_2O or CH_4) flow rate $Q_a = 0.5 \text{ l/min}$. The concentration maxima at $V_m = 0.18 \text{ m/s}$ are normalized to 1.

3.3 Visualization of the flows in the CDRS reactor

The image of the flow structure in the CDRS reactor when a positive voltage of 28 kV was applied is shown in Fig. 4. As it can be seen, there exists a strong secondary flow in the upstream region of the CDRS reactor, with at least two well-marked vortexes at a distance 6–12 cm from the nozzle. The flow structure observed in the upstream region results from the interaction between the gas ionic current emanating from the stressed electrode towards the collecting electrodes and the additional and main gas flows. However, visualization of the additional flow when no voltage was applied showed that the additional gas jet does not penetrate deep

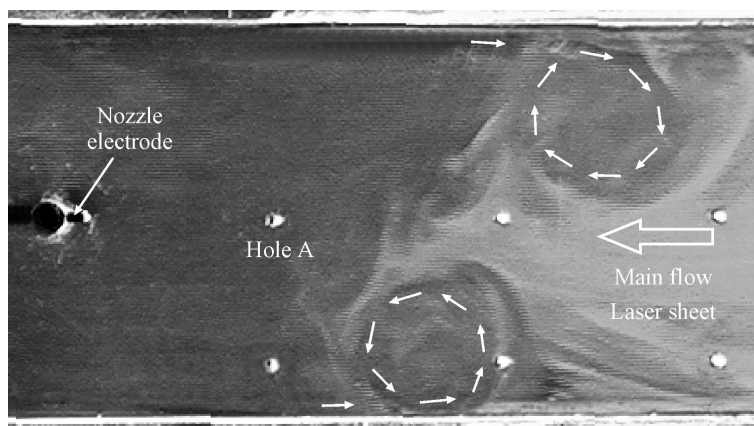


Fig. 4. Image (side view) of the flow structure in the CDRS reactor when a positive voltage of 28 kV was applied (averaged discharge current 150 μA). The main gas flow velocity $V_m = 0.18$ m/s, the additional flow rate $Q_a=0.5$ l/min. The distance between the nozzle electrode tip and the hole A is 43 mm. The other holes (made in the acrylic side-wall for gas sampling) are seen.

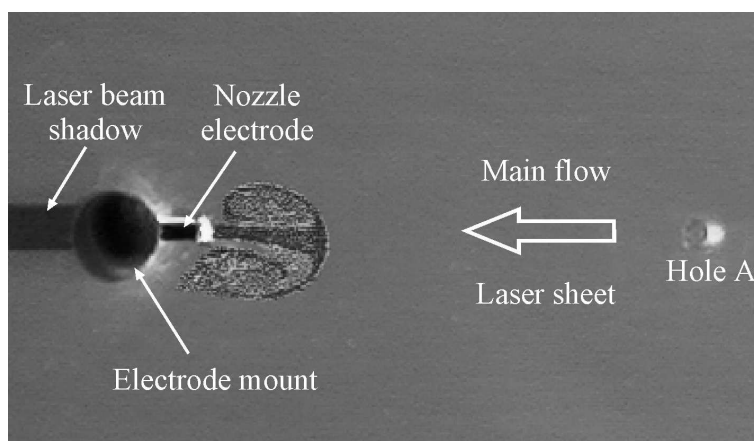


Fig. 5. Image (side view) of the additional flow structure for additional gas flow rate of $Q_a = 0.5$ l/min. The main gas flow velocity $V_m = 0.18$ m/s. No voltage applied. The distance between the nozzle electrode tip and the hole A (made for gas sampling) is 43 mm. The main flow was air (seeded with cigarette smoke) and the additional flow was ambient air (unseeded).

upstream (Fig. 5). Thus, one may infer that the secondary flow in the upstream region of the CDRS reactor is mainly a result of the EHD forces. As measured in the similar electrode arrangements (a conventional needle-to-plate non-thermal plasma reactor [7], model of the electrode precipitator [11]), the EHD flow can be as fast as 2.5 m/s in the discharge area and about 0.6 m/s at a distance 10 cm from

the discharge electrode upstream. Such velocities are higher or comparable to that of the main gas flow. Thus, the EHD flow has a momentum high enough to drift ozone molecules against the main gas flow, becoming the dominant factor of ozone molecules transport upstream of the discharge region.

4 Discussion and conclusions

To our knowledge, this investigation showed for the first time that ozone molecules produced by the streamer corona discharge in the CDRS reactor are transported not only in the downstream region, but also in the upstream region of the CDRS reactor. The EHD secondary flow is responsible for the ozone transport upstream of the discharge region. The finding of ozone molecules (and presumably other long-living active species) far outside the discharge region may have an impact on modelling and optimising the chemical kinetics as well as designing the non-thermal plasma reactors. The modelling of the chemical kinetics of species in the non-thermal plasma reactor should also comprise the processes outside the discharge region. This may require taking into consideration the gas flow and corresponding transport of the active species, which both have been neglected.

The presence of ozone molecules in the upstream region of the non-thermal plasma reactor, proved in this experiment, helps in elucidating Ohkubo et al. [1] and Kanazawa et al. [2] observation of NO removal in the upstream region of the reactor. At very low main gas velocity as in [1, 2], i.e. 2 mm/s, the concentration of ozone molecules in the upstream region of the reactor can be relatively high. As a result, the NO molecules can be converted in NO₂ molecules already in the upstream region, showing the significant NO removal before the discharge region. Therefore, the supposition made in [7] that ozone molecules are responsible for NO molecules decomposition in the upstream region of the non-thermal plasma reactor seems to be confirmed in this experiment.

Another conclusion is that the transport of ozone molecules (and presumably other active species) outside the discharge zone can enhance the gaseous pollutant removal in the non-thermal plasma reactors. Hence, apart from the discharge zone also other regions of the reactor can be important for the processing of gaseous pollutants.

The support by the Foundation for Polish Science (Fundacja na Rzecz Nauki Polskiej, subsidy 8/2001), the Institute of Fluid Flow Machinery, Polish Academy of Sciences, Gdańsk (grant IMP PAN O3/Z-3/T2), the State Committee for Research and Development (grant PB 0446/T09/20/19) and the Canadian-Japanese-Polish Scientific Cooperation are highly appreciated. J. Mizeraczyk is indebted to Dr. N.J. Mason, Prof. J.D. Skalny, Dr. S. Pekarek, Dr. M. Simek and Dr. P. F. Pontiga for helpful discussions at the NATO Project (Project PST CLG 976544) meetings in London and Bratislava.

References

- [1] T. Ohkubo, S. Kanazawa, Y. Nomoto, J. Mizeraczyk: in *35th Annual Meeting – IEEE Industry Applications Society* (IEEE Industry Applications Society), Roma, Italy, 2000, vol. 1&2, 864–867
- [2] S. Kanazawa, Y. Shuto, N. Sato, T. Ohkubo, Y. Nomoto, J. Mizeraczyk, J. S. Chang: submitted to the *IEEE Transactions on Industrial Applications* (2001)
- [3] L. B. Loeb: *Electrical Coronas*, Ed. Berkeley C.A., University of California Press, 1965, 402–407
- [4] T. Yamamoto, H. R. Velkoff: *J. Fluid Mech.* **108** (1981) 1–18
- [5] P. Atten, F. M. J. McCluskey, A. C. Lahjomri: *IEEE Trans., Indust. Appl.* **23** (1987) 705–711
- [6] J. Mizeraczyk, M. Kocik, J. Dekowski, M. Dors, J. Podliński, T. Ohkubo, S. Kanazawa, T. Kawasaki: *J. Electrostatics* **51–52** (2001) 272–277
- [7] J. Mizeraczyk, J. Dekowski, J. Podliński, M. Dors, M. Kocik, J. Mikielwicz, T. Ohkubo, S. Kanazawa: *IEEE Trans. on Plasma Science* **30** (2002)
- [8] A. C. Gentile, M. J. Kushner: *J. Appl. Phys.* **78** (1995) 2074–2085
- [9] J. J. Lowke, R. Morrow: *IEEE Trans. Plasma Sci.* **23** (1995) 661–671
- [10] E. A. Filimonova, R. H. Amirov, H. T. Kim, I. H. Park: *J. Phys. D: Appl. Phys.* **33** (2000) 1716–1727
- [11] K. Yan, T. Yamamoto, S. Kanazawa, T. Ohkubo, Y. Nomoto, J. S. Chang: *J. Electrostatics* **46** (1999) 207–219
- [12] M. Kocik, J. Podliński, J. Dekowski, J. Mizeraczyk: in: *Proc. SPIE vol. 4238, Laser Technology VI: Applications* (Wiesław L. Woliński, Zdzisław Jankiewicz) Świnoujście, Poland, 2000, 246–249